series therefore converges for all

$$\lambda<1\Big/\left[4\int_1^\infty \frac{\sigma(x)dx}{m_0+x}\right]. \tag{11}$$

## CONCLUSIONS

It is apparent that the argument for the convergence of the series making up the proper vertex part goes through exactly as with the proper self-energy parts provided $E\leq m_0$. For $E>m_0$ the argument above requires rethinking because of the tendency for cancellation in the denominators. We have not bothered with this point because of its irrelevance to the basic questions of existence of a solution and convergence at the points necessary for renormalization.

It is not surprising that we have found convergence in the case considered in view of the fact that, for example, in neutral scalar theory the fields correspond to a harmonic oscillator with a linear perturbation in contrast to the anharmonic systems which are qualitatively very different for large $\langle\phi\rangle$.

Finally, we would like to point out that the models covered by this proof are nontrivial as compared to such truncated models as the Lee model in which the series for $\Sigma(0,m_0)$ consists of one term.

## ACKNOWLEDGMENT

It is a pleasure to thank Professor Cornel Eftimiu, University of Missouri–St. Louis, for invaluable discussions.

PHYSICAL REVIEW D VOLUME 2, NUMBER 4 15 AUGUST 1970

# Renormalization and Unitarity in the Dual-Resonance Model*

DAVID J. GROSS, A. NEVEU,† J. SCHERK,‡ AND JOHN H. SCHWARZ
*Joseph Henry Laboratories, Princeton University, Princeton, New Jersey 08540*

(Received 26 March 1970)

All the one-loop graphs of the dual-resonance model are explicitly calculated. These graphs fall into three categories: planar, nonorientable, and orientable nonplanar. Using the properties of various elliptic functions, we are able to generalize the renormalization procedure, obtained previously for the planar diagrams, to the other two categories. The orientable nonplanar diagrams turn out to be particularly interesting. First, their integration regions have to be reduced from the ones naively obtained in order to avoid multiple counting. Secondly, they give rise to new singularities (branch points) in channels that are naturally identified as having vacuum quantum numbers. These singularities are probably related to the Pomeranchukon. The question of unitarity is explored at the one-loop level, i.e., to the first nontrivial order in the perturbation series. Although the counting of diagrams is somewhat subtle, a rather simple result emerges: All inequivalent diagrams (with respect to duality transformations) should be counted with equal weight. Finally, it is indicated that three of the four primitive renormalized loop operators of the theory can be obtained from the formulas of this paper.

## I. INTRODUCTION

AN attractive attitude towards the generalized Veneziano model[1,2] is that it provides one with the Born approximation to a theory of hadrons. The The implementation of this idea is seemingly straightforward. One proceeds to factorize the Born term,[3] i.e., the $N$-point tree graphs, thereby deducing the level structure implicit in the model and the Feynman rules of the theory.[4] These rules are then to be utilized in the construction of a unitary perturbation series.

The one-loop planar diagrams were in fact easily derived[5] once it had been demonstrated that the tree graphs were completely factorizable.[3] Further progress has, however, been impeded by a series of technical difficulties and by the fundamental problem of renormalization. The technical difficulties relate to the inclusion of twisted vertices and to the removal of the spurious states which are found by naive factorization.

The twisted vertices are necessary for the construction of twisted loop diagrams, some of which correspond to nonplanar Feynman graphs and some of which (the

* Supported in part by the U. S. Air Force Office of Scientific Research, under Contract No. AF-49(638)-1545.

† Procter Fellow.

‡ NATO Fellow, on leave of absence from Laboratoire de Physique Théorique, Orsay, France.

[1] G. Veneziano, Nuovo Cimento **57A**, 190 (1968).

[2] C. J. Goebel and B. Sakita, Phys. Rev. Letters **22**, 256 (1969); C. H. Mo and T. S. Tsun, Phys. Letters **28B**, 485 (1969); K. Bardakci and H. Ruegg, Phys. Rev. **181**, 1884 (1969); Z. Koba and H. B. Nielson, Nucl. Phys. **B10**, 633 (1969).

[3] S. Fubini and G. Veneziano, Nuovo Cimento **64A**, 811 (1969); K. Bardakci and S. Mandelstam, Phys. Rev. **184**, 1640 (1969).

[4] S. Fubini, D. Gordon, and G. Veneziano, Phys. Letters **29B**, 679 (1969); Y. Nambu, University of Chicago report, 1969 (unpublished).

[5] K. Bardakci, M. B. Halpern, and J. A. Shapiro, Phys. Rev. **185**, 1910 (1969); D. Amati, C. Bouchiat, and J. L. Gervais, Nuovo Cimento Letters **2**, 399 (1969).

so-called nonorientable graphs) have no corresponding analog in Feynman theory. Such diagrams are, in general, required in order to satisfy unitarity. Twists can be handled with relative ease by defining a twist operator[6,7] which takes one from untwisted vertices to twisted ones. The spurious states appear in the factorization of the tree graphs due to linear dependences among the vertices (the so-called Ward identities[3]). There exist, therefore, linear combinations of the states used in the factorization that do not couple to the external scalar particles and give no contribution to the full tree amplitudes. It is possible to explicitly remove them from the model by defining a projection operator onto the subspace of real states.[8] There is a great advantage to working within this projected subspace, since one can then replace any operator in the theory by another one which has identical matrix elements in the subspace of real states (these are related by the so-called gauge transformations).

The planar one-loop amplitudes exhibit an exponential divergence, which is directly related to the enormous number of states in the theory. Two of us[9] have shown how to construct a counter term that cancels this divergence, while preserving duality, perturbative unitarity, Regge behavior, and factorization.[10]

In this paper, using the techniques described above, we consider the complete set of twisted and untwisted one-loop amplitudes. We carry out the sums over the intermediate states that appear in the loops and reduce the general one-loop amplitude to an integral over elliptic functions. The planar and nonorientable diagrams are renormalized by constructing appropriate counter terms. The nonplanar orientable diagrams are shown to be finite in a certain region of the energy plane but probably require renormalization, too. These amplitudes develop branch points in an energy variable that are unrelated to normal thresholds. We think that these singularities, which are specific to the vacuum channel, are related to the Pomeranchukon, but at the present time we are not sure how to treat them. Finally, we discuss the question of unitarity at the one-loop level. More specifically, we determine the set of $N$-particle one-loop graphs that is unitary to this order in the coupling constant. It turns out that a unitary result is obtained when all graphs that are not related by a duality transformation are summed with equal weight.

It might appear that the calculation of the one-loop amplitudes is only the first step in the infinite procedure of evaluating the sum of all diagrams necessary for unitarity. This, however, is not the case in a dual theory. Recently, we have[11] analyzed the general $N$-point diagram for any dual theory and have shown that there are only the four one-particle irreducible diagrams shown in Fig. 1. Any dual Feynman diagram can be constructed, once one knows the four operators which these graphs represent, by attaching appropriate numbers of such graphs onto a tree diagram. Moreover, it is possible that the (formal) sum of all the diagrams required by unitary can be written explicitly in terms of these four operators. Since three of them are one-loop operators, they can be derived by factorizing the general one-loop planar [Fig. 1(a)], nonorientable [Fig. 1(b)], and orientable nonplanar [Fig. 1(c)] diagrams. In Ref. 10 this procedure was carried out explicitly for the self-energy operator related to the planar tadpole [Fig. 1(a)]. Furthermore, counterterm operators for Figs. 1(a) and 1(b) can easily be derived.[10] The solution of the one-loop problem contains, therefore, three of the four operators which are required to construct the full unitary theory.

Finally, we are considering a model with no internal degrees of freedom, and with several undesirable properties (ghosts, negative-intercept trajectories, lack of fermions, etc.). There are indications[12,13] that more realistic models can be constructed by suitable alterations of the Born term. It is unlikely, however, that these will change in any fundamental way the dynamics of the loop amplitudes considered in this paper.

In Sec. II we review the algebraic methods necessary for the calculation of loop diagrams, especially the methods used for treating twists and spurious state projections. The sum over intermediate states in the general loop integral is explicitly carried out. Section III is devoted to a short review of the planar diagrams, and their renormalization. Section IV deals with the nonorientable diagrams. These are calculated and renormalized. In Sec. V we calculate the nonplanar orientable diagrams. It is shown that naive application of the Feynman rules involves an infinite counting, which can, however, be easily remedied. The new singularities generated by this diagram are discussed. In Sec. VI we discuss the unitarity of the $N$-point one-loop diagrams. The Appendix contains a discussion of the elliptic functions that appear in the loop integrals.

## II. PROJECTIONS, TWISTS, AND DIAGONALIZATION OF TRACES

In this section we review the algebraic methods that have been developed for calculating the $N$-point one-

[6] L. Caneschi, A. Schwimmer, and G. Veneziano, Phys. Letters **30B**, 351 (1969).
[7] D. Amati, M. Le Bellac, and D. Olive, Nuovo Cimento **66A**, 815 (1970); **66A**, 831 (1970); F. Gliozzi, Nuovo Cimento Letters **2**, 846 (1969); C. B. Chiu, S. Matsuda, and C. Rebbi, Phys. Rev. Letters **23**, 1526 (1969).
[8] C. B. Thorn, Phys. Rev. D **1**, 1693 (1970); M. Kaku and C. B. Thorn, *ibid.* **1**, 2860 (1970); R. Brower and J. Weis, Nuovo Cimento Letters **3**, 285 (1970).
[9] A. Neveu and J. Scherk, Phys. Rev. D **1**, 2355 (1970); G. Frye and L. Susskind, Phys. Letters **31B**, 537 (1970).
[10] T. H. Burnett, D. J. Gross, A. Neveu, J. Scherk, and J. H. Schwarz, Phys. Letters **32B**, 115 (1970).
[11] D. J. Gross, A. Neveu, J. Scherk, and J. H. Schwarz, Phys. Letters **31B**, 592 (1970).
[12] M. A. Virasoro, Phys. Rev. D **1**, 2933 (1970).
[13] K. Bardakci and M. Halpern, Phys. Rev. Letters **24**, 428 (1970).

loop integral with an arbitrary number of twisted lines. We also show explicitly the algebra required to remove the contribution of spurious states that do not appear in the primitive $N$-point functions. Almost all the techniques and results of this section can be found in Refs. 4–8, especially the work of Kaku and Thorn. It should be helpful, however, to have the salient facts all collected in one place.

We begin by recalling that the level structure of the dual-resonance model is described by vectors in a Hilbert space generated by an infinite number of four-vector creation operators, $a_n^{\dagger\mu}$, $n=1, 2, \ldots$.[4] The propagator for momentum $p$ is given by the operator

$$D(R,p)=\int_0^1 dx(1-x)^{\alpha_0-1}x^{R-\alpha(p^2)-1}, \qquad (2.1)$$

where

$$R=\sum_{n=1}^{\infty} n a_n^{\dagger}\cdot a_n$$

and one has linear trajectory functions

$$\alpha(s)=\alpha_0+\tfrac{1}{2}s.$$

The vertex operator for coupling an on-shell scalar state of momentum $k$ [with $\alpha(k^2=m^2)=0$] is

$$V(k)=g\exp\left(\sum_{n=1}^{\infty}\frac{k\cdot a_n^{\dagger}}{\sqrt{n}}\right)\exp\left(\sum_{n=1}^{\infty}\frac{k\cdot a_n}{\sqrt{n}}\right). \qquad (2.2)$$

These operators are sufficient to reproduce the standard $N$-point functions in any multiperipheral configuration.

We now introduce the three additional operators ($p^2=m^2$ in our metric)

$$\begin{aligned} L_0(p)&=R-\tfrac{1}{2}p^2,\\ L_+(p)&=p\cdot a_1^{\dagger}+\sum_{n=1}^{\infty}[n(n+1)]^{1/2}a_{n+1}^{\dagger}\cdot a_n,\\ L_-(p)&=-p\cdot a_1+\sum_{n=1}^{\infty}[n(n+1)]^{1/2}a_n^{\dagger}\cdot a_{n+1}. \end{aligned} \qquad (2.3)$$

These three operators generate the algebra $SU(1,1)$[7]:

$$[L_0,L_{\pm}]=\pm L_{\pm},\quad [L_+,L_-]=-2L_0. \qquad (2.4)$$

Next, define

$$\begin{aligned} A(p)&\equiv A=L_0(p)-L_-(p),\\ A^{\dagger}(-p)&\equiv A^{\dagger}=L_0(p)-L_+(p). \end{aligned}$$

$A^{\dagger}(p)$ has been constructed in such a way as to create, when applied to any state in the Hilbert space, "spurious" states that do not couple to any number of external scalar particles. Therefore, one has the option of removing such states from the theory.[14] This is done by introducing the projection operator[8]

$$P=I-(A^{\dagger}-\alpha_0)[A(A^{\dagger}-\alpha_0)]^{-1}A, \qquad (2.5)$$

which satisfies

$$\begin{aligned} D(R,p)P(p)&=P^{\dagger}(-p)D(R,p),\\ P(p+k)V(k)&=V(k)P^{\dagger}(-p). \end{aligned} \qquad (2.6)$$

The projected propagator $P^{\dagger}(-p)D(R,p)P(p)$ is Hermitian and contains states which have linearly independent couplings to external scalar particles.

The twist operator of Caneschi, Schwimmer, and Veneziano[6] is given by

$$\Omega=(-1)^R e^{-L_+}=e^{(1-\beta)L_+}(-1)^R e^{-\beta L_+}, \qquad (2.7)$$

where the second form is made possible by the general rule

$$x^{L_0}f(L_+)=f(xL_+)x^{L_0}. \qquad (2.8)$$

This twist is unique only up to a gauge transformation generated by $A$. It is shown in Ref. 7 that the choice

$$\Theta(z)=\Omega(1-z)^A=(1-z)^{-A}\Omega, \qquad (2.9)$$

where $z$ is the integration variable of the adjacent propagator ($\Theta$ is brought inside the integral), has the desirable Hermiticity property

$$z^R\Theta(z)=\Theta^{\dagger}(z)z^R. \qquad (2.10)$$

The last formula guarantees that the result of a calculation does not depend on the placement of dots; i.e., twisting on both sides of a propagator is equivalent to not twisting at all.

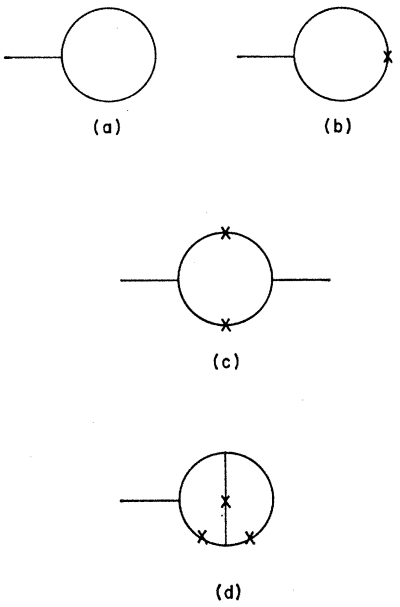


FIG. 1. The four primitive graphs of the dual-resonance theory.

[14] This is highly desirable since otherwise one must enlarge the Hilbert space, by introducing additional scalar modes, in order to achieve factorization of the twisted vertices (see Amati *et al.*, Ref. 7). With the projections one never needs to introduce additional scalar modes.

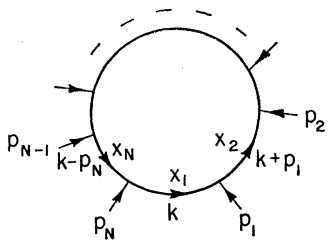


FIG. 2. General one-loop diagram in the configuration where the external lines are attached directly to the loop.

Recording two more useful identities proved by Thorn,[8]

$$A(p+k)V(k)D(R,p)=V(k)D(R+1,p)A(p), \quad (2.11)$$

$$A(p)\Omega(p)=-\Omega(p)A(p), \quad (2.12)$$

we may proceed to the calculation of traces. The problem is to calculate a diagram of the form shown in Fig. 2 in which an arbitrary number of the internal lines are twisted. The corresponding integral (aside from modifications to be discussed in subsequent sections) is

$$\int d^4k\ \mathrm{Tr}\{V(p_1)P^\dagger(k+p_1)D(R,k+p_1)[1+\Theta(k+p_1)]$$
$$\times P(-k-p_1)V(p_2)P^\dagger(k+p_1+p_2)\cdots V(p_N)$$
$$\times P^\dagger(k)D(R,k)[1+\Theta(k)]P(-k)\}.$$

We have introduced a factor $1+\Theta$ for each line. What we really mean is to choose 1 or $\Theta$ for each line depending on which lines are to be twisted. The commutation and projection properties of $P$ enable one to replace $\Theta$'s by $\Omega$'s and drop all but one of the projections in the trace, leaving us with

$$\mathrm{Tr}\{V(p_1)D(R,k+p_1)[1+\Omega(k+p_1)]V(p_2)\cdots V(p_N)$$
$$\times D(R,k)[1+\Omega(k)]P(-k)\}.$$

Finally, bringing the $A$ on the right of $1-P$ around through the trace gives[8]

$$\mathrm{Tr}\{V(p_1)D(R,k+p_1)[1+\Omega(k+p_1)]$$
$$\times V(p_2)\cdots V(p_N)D(R,k)[1+\Omega(k)]\}$$
$$-\mathrm{Tr}\{V(p_1)D(R+1,k+p_1)[1-\Omega(k+p_1)]$$
$$\times V(p_2)\cdots V(p_N)D(R+1,k)[1-\Omega(k)]\}.$$

Therefore, we conclude that for a particular choice of $M$ twists one has

$$[1-(-1)^M w]\ \mathrm{Tr}\{V(p_1)D(R,k+p_1)[1\text{ or }\Omega(k+p_1)]$$
$$\times V(p_2)\cdots V(p_n)D(R,k)[1\text{ or }\Omega(k)]\}, \quad (2.13)$$

where

$$w=\prod_{i=1}^{N} x_i,$$

and $x_i$ is the integration variable of the $i$th propagator.

The factor $1\pm w$ is understood, of course, to be brought inside the propagator integrals. The problem of the projection is thus completely solved and the next question is how to calculate the traces.

The trace calculation is completely straightforward, using the properties of coherent states, when only vertices and diagonal operators appear.[5] When one or more twists are also present, such a form is not manifest. Therefore, for the configuration of Fig. 3, we now show how to reduce the trace to a form which is as simple as the one without twists. The restriction to $M\geqslant 1$ adjacent twisted lines is strictly for convenience; the generalization will be made evident. Dropping the nonoperator parts of the trace and writing the twist operators in the second form of Eq. (2.7), we wish to calculate

$$\mathrm{Tr}\{x_1{}^R\Omega_{\beta_1}Vx_2{}^R\Omega_{\beta_2}\cdots x_M{}^R\Omega_{\beta_M}Vy_1{}^RV\cdots y_N{}^RV\}.$$

The key equation required to simplify the algebra is

$$e^{\beta L_+}=(1+\beta)^{L_0}(1+\beta)^{L_+-L_0}. \quad (2.14)$$

This relation is proved by first showing

$$F(1+\beta)=(1+\beta)^{L_+-L_0}=e^{L_+}(1+\beta)^{-L_0}e^{-L_+}, \quad (2.15)$$

which is true because both sides have the group property $F(\gamma_1)F(\gamma_2)=F(\gamma_1\gamma_2)$, and the infinitesimal operators are easily seen to agree. Equation (2.15) is then combined with

$$(1+\beta)^{L_0}e^{L_+}=e^{(1+\beta)L_+}(1+\beta)^{L_0}, \quad (2.16)$$

which is a special case of Eq. (2.8), to give Eq. (2.14). The additional relations

$$(1-\beta)^{\alpha_0-A^\dagger(-p-k)}V(k)=V(k)(1-\beta)^{-A^\dagger(-p)} \quad (2.17)$$

and

$$e^{-\beta L_+}x^R=x^Re^{-\beta L_+/x} \quad (2.18)$$

provide all the algebraic tools needed.

Equations (2.7), (2.14), (2.17), and (2.18) may be

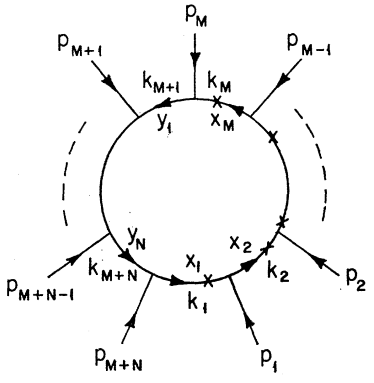


FIG. 3. One-loop diagram having $M$ adjacent twisted internal lines and $N$ adjacent untwisted internal lines.

combined to show that

$$\Omega_\beta V x^R = e^{(1-\beta)L_+}(-1)^R(1-\beta)^{L_0-\alpha_0}V(1-\beta)^{-L_0} \times x^R e^{-\beta L_+/x}. \quad (2.19)$$

This relation is used repeatedly for every twist in the trace. The $\beta$'s, which until now were arbitrary, are then chosen to cancel the $L_+$'s occurring in the exponentials. This cancellation requires that

$$\frac{\beta_1}{x_2}=1-\beta_2, \quad \frac{\beta_2}{x_3}=1-\beta_3, \ldots,$$

$$\frac{\beta_{M-1}}{x_M}=1-\beta_M, \quad \frac{\beta_M}{y_1y_2\cdots y_N x_1}=1-\beta_1.$$

It then follows that the operator part of the remaining trace is

$$\mathrm{Tr}\{(-u_1)^R V(-u_2)^R\cdots(-u_M)^R \times V v_1{}^R V\cdots v_N{}^R V\}, \quad (2.20)$$

where

$$u_1=\frac{\beta_M}{y_1y_2\cdots y_N-\beta_M}, \quad u_2=\frac{\beta_1}{1-\beta_1}, \ldots, \quad u_M=\frac{\beta_{M-1}}{1-\beta_{M-1}}, \quad (2.21)$$

and

$$v_1=\frac{y_1-\beta_M}{1-\beta_M}, \quad v_2=\frac{y_1y_2-\beta_M}{y_1-\beta_M}, \ldots, \quad v_N=\frac{y_1y_2\cdots y_N-\beta_M}{y_1y_2\cdots y_{N-1}-\beta_M}. \quad (2.22)$$

Eliminating the $\beta$'s between Eqs. (2.21) and (2.22) yields

$$x_1=\frac{u_1(1+u_2)}{1+u_1}, \quad x_2=\frac{u_2(1+u_3)}{1+u_2}, \ldots, \quad x_{M-1}=\frac{u_{M-1}(1+u_M)}{1+u_{M-1}}, \quad x_M=\frac{u_M(1+v_1v_2\cdots v_Nu_1)}{1+u_M}, \quad (2.23)$$

and

$$y_1=\frac{v_1+v_1v_2\cdots v_Nu_1}{1+v_1v_2\cdots v_Nu_1}, \quad y_2=\frac{v_2+v_2v_3\cdots v_Nu_1}{1+v_2v_3\cdots v_Nu_1}, \ldots, \quad y_N=\frac{v_N+v_Nu_1}{1+u_1}. \quad (2.24)$$

Note that the product of $u$'s and $v$'s is the same as the product of $x$'s and $y$'s,

$$w=\prod_{i=1}^{M}x_i\prod_{j=1}^{N}y_j=\prod_{i=1}^{M}u_i\prod_{j=1}^{N}v_j.$$

The Jacobian for changing from $x$ and $y$ integrations to $u$ and $v$ integrations is

$$\prod_{i=1}^{M}dx_i\prod_{j=1}^{N}dy_j=[1-(-1)^Mw]\times\prod_{i=1}^{M}\frac{du_i}{1+u_i}\prod_{j=1}^{N}\frac{dv_j}{1+v_jv_{j+1}\cdots v_Nu_1}.$$

Finally, collecting factors that have been dropped along the way, we may assemble the formula for the loop integral with $M$ adjacent twists,

$$F_{N,M}=\int d^4k\int[\prod_{i=1}^{M}du_iu_i{}^{-\alpha(k_i^2)-1}][\prod_{j=1}^{N}dv_jv_j{}^{-\alpha(k_j+M^2)-1}] \times[1-(-1)^Mw]^2[(1-u_Mv_1v_2\cdots v_Nu_1) \times\prod_{i=1}^{M-1}(1-u_iu_{i+1})\prod_{j=1}^{N}(1-v_j)]^{\alpha_0-1} \times\mathrm{Tr}\{(-u_1)^RV(p_1)(-u_2)^R\cdots(-u_M)^R \times V(p_M)v_1{}^RV(p_{M+1})\cdots v_N{}^RV(p_{M+N})\}. \quad (2.25)$$

We have now accomplished the goal of rewriting the loop integral in a form for which the trace calculations are no worse in twisted configurations than in untwisted ones. Superficially, at least, the upper limits of the $u$ and $v$ integrations correspond to the zeros of the factors that appear to the power $\alpha_0-1$. This rule will be modified in later sections.

The general rule for a one-loop diagram in the configuration of Fig. 3 with $M$ arbitrarily placed twisted lines is now quite evident. (1) Jacobians and projections contribute a factor $[1-(-1)^Mw]^2$ except when $M=0$, in which case the factor is just $1-w$. (2) Each line gives a factor $u^{-\alpha(k^2)-1}$ (where $u$ is a twisted line of momentum $k$) or $v^{-\alpha(k^2)-1}$ (where $v$ is an untwisted line of momentum $k$). (3) There is a trace in which the lines and vertices appear in cyclic order with an untwisted line giving $v^R$, and a twisted line giving $(-u)^R$. (4) The following factors appear to the power $\alpha_0-1$: a factor $(1-v_i)$ for each untwisted line $v_i$, and a factor of the form $(1-u_kv_lv_{l+1}\cdots v_{l+m}u_{k+1})$, where $u_k$ and $u_{k+1}$ refer to two successive twisted lines with $m+1$ intervening untwisted lines, for each twisted line $u_k$. In the particular case of just one twisted line, the last factor becomes $1-uw$. (5) Finally, the $u$'s and $v$'s are integrated over the region in which they are positive and in which the factors given above are also positive. This rule will be modified in Sec. V in the case where $M$ is even and nonzero.

## III. PLANAR DIAGRAMS

In order to deal with the simplest case first, we consider the $N$-point loop with no twists. The rules of Sec. II give for this case

$$F_N=\int d^4k\int_0^1\prod_{i=1}^{N}[dx_i(1-x_i)^{\alpha_0-1}x_i^{-\alpha(k_i^2)-1}](1-w)\mathcal{T}, \tag{3.1}$$

where, using the techniques of Amati *et al.*[5] to evaluate the trace,

$$\mathcal{T}=\mathrm{Tr}\{x_1{}^R V(p_1)x_2{}^R\cdots x_N{}^R V(p_N)\}$$
$$=g^N[f(w)]^{-4}\prod_{i,j=1}^{N}\prod_{n=1}^{\infty}\exp\left[\frac{p_i\cdot p_j C_{ji}{}^n}{n(1-w^n)}\right], \tag{3.2}$$

$$f(w)=\prod_{n=1}^{\infty}(1-w^n),$$

$$C_{ji}=x_{i+1}x_{i+2}\cdots x_j \text{ (in cyclic order)}.$$

Thus, since $C_{ii}=w$ and $C_{ij}=w/C_{ji}$ for $i\neq j$,

$$\mathcal{T}=g^N[f(w)]^{-4}\prod_{n=1}^{\infty}\left\{\prod_{1\leqslant i<j\leqslant N}\exp\left[p_i\cdot p_j\frac{C_{ji}{}^n+(w/C_{ji})^n}{n(1-w^n)}\right]\prod_{i=1}^{N}\exp\left[p_i{}^2\frac{w^n}{n(1-w^n)}\right]\right\}$$
$$=g^N[f(w)]^{-4}\prod_{n=1}^{\infty}\prod_{1\leqslant i<j\leqslant N}\exp\left[p_i\cdot p_j\frac{C_{ji}{}^n+(w/C_{ji})^n-2w^n}{n(1-w^n)}\right],$$

where the last step uses momentum conservation. We can now recognize the infinite products as Jacobi $\theta$ functions. Using

$$\theta_1\left(\frac{\ln x}{2\pi i}\middle|\frac{\ln w}{2\pi i}\right)=ix^{-1/2}f(w)w^{1/8}\prod_{n=0}^{\infty}(1-xw^n)(1-w^{n+1}/x),$$

we find that

$$\mathcal{T}=g^N[f(w)]^{-4}\prod_{1\leqslant i<j\leqslant N}\left[-2\pi iC_{ji}{}^{1/2}\theta_1\left(\frac{\ln C_{ji}}{2\pi i}\middle|\frac{\ln w}{2\pi i}\right)\Big/\theta_1'\left(0\middle|\frac{\ln w}{2\pi i}\right)\right]^{-p_i\cdot p_j}$$
$$=g^N[f(w)]^{-4}\left(\frac{w}{x}\right)^{-\alpha_0}\left(\prod_{i=2}^{N-1}x_{i+1}{}^{-\alpha_{1i}}\right)\prod_{1\leqslant i<j\leqslant N}\left[-2\pi i\theta_1\left(\frac{\ln C_{ji}}{2\pi i}\middle|\frac{\ln w}{2\pi i}\right)\Big/\theta_1'\left(0\middle|\frac{\ln w}{2\pi i}\right)\right]^{-p_i\cdot p_j}, \tag{3.3}$$

where the derivatives refer to the first variable of the $\theta_1$ function, a standard notation.

The momentum integration is now required for putting $F_N$ into the desired form. Following tradition, we do not discuss the validity of the Wick rotation that is needed.

$$\mathfrak{M}=\int d^4k\prod_{i=1}^{N}x_i^{-\alpha(k_i^2)-1}$$
$$=\frac{4\pi^2}{\ln^2 w}w^{-\frac{1}{2}\alpha_0-1}\exp\left(\frac{\alpha_0}{2\ln w}\sum_{i=1}^{N}\ln^2(x_i)\right)\exp\left(-\sum_{1\leqslant i<j\leqslant N-1}\alpha_{ij}\frac{\ln x_i\ln x_{j+1}}{\ln w}\right)$$
$$=\frac{4\pi^2}{w\ln^2 w}x_1{}^{-\alpha_0}\left(\prod_{i=2}^{N-1}x_{i+1}{}^{-\alpha_{1i}}\right)\prod_{1\leqslant i<j\leqslant N}\exp\left(-\frac{p_ip_j\ln^2 C_{ji}}{2\ln w}\right). \tag{3.4}$$

To carry out the last step in the algebra of (3.4), it is useful to know that momentum conservation and the mass-shell constraint allow one to prove the general rule

$$\prod_{1\leqslant i<j\leqslant N-1}\left(\frac{B_{i,j}B_{i-1,j+1}}{B_{i,j+1}B_{i-1,j}}\right)^{-\alpha_{ij}}$$
$$=\left(\prod_{i=1}^{N}B_{i-1,i}{}^{\alpha_0}\right)\left(\prod_{1\leqslant i<j\leqslant N}B_{i,j}{}^{-p_i\cdot p_j}\right),$$

where one defines $B_{0,j}\equiv B_{j,N}$. [In using this rule in (3.4), the $i=1$ terms require special care.] Inserting (3.3) and (3.4) into (3.1), we obtain

$$F_N=4\pi^2g^N\int\prod_{i=1}^{N}[dx_i(1-x_i)^{\alpha_0-1}]$$
$$\times\frac{w^{-\alpha_0-1}[f(w)]^{-4}}{\ln^2 w}\prod_{1\leqslant i<j\leqslant N}[\psi(C_{ji})]^{-p_i\cdot p_j}, \tag{3.5}$$

where

$$\psi(x)=\psi(x,w)=-2\pi i$$
$$\times\exp\left(\frac{\ln^2 x}{2\ln w}\right)\theta_1\left(\frac{\ln x}{2\pi i}\middle|\frac{\ln w}{2\pi i}\right)\Big/\theta_1'\left(0\middle|\frac{\ln w}{2\pi i}\right). \tag{3.6}$$

Several properties of $\psi(x)$ are discussed in the Appendix. In particular, we note the property $\psi(x)=\psi(w/x)$. This means that for a particular term with exponent $p_i\cdot p_j$ the argument of the $\psi$ function is the product of the $x$ variables that appear between the two momenta, and it does not matter on which side these $x$'s are chosen. One immediate consequence of this invariance is the cyclic symmetry of $F_N$ in the external momenta.

As has already been exhaustively discussed in the literature, $F_N$ has an exponential divergence as $w\to 1$, which is entirely attributable to the factor $[f(w)]^{-4}$. A useful formula for displaying this divergence, which is a corollary of the $\theta$-function transformations discussed in the Appendix, is

$$\frac{4\pi^2}{\ln^2 w}[f(w)]^{-4}=w^{1/6}q^{-1/3}[f(q^2)]^{-4}, \tag{3.7}$$

where

$$q=\exp(2\pi^2/\ln w).$$

It is shown in the Appendix that

$$\tilde{\psi}(x)=-\frac{\ln w}{\pi}\sin\left(\frac{\pi\ln x}{\ln w}\right) \tag{3.8}$$

differs from $\psi(x)$ by $O(q^2)$ as $w\to 1$. Therefore, if we construct $\tilde{F}_N$ by replacing $\psi$ by $\tilde{\psi}$ in (3.5), the difference $F_N-\tilde{F}_N$ is finite. The duality and analyticity properties of $\tilde{F}_N$ that allow it to be interpreted as an acceptable counterterm have been discussed in Ref. 9. The demonstration that it can be consistently factorized was given in Ref. 10. We emphasize that $\tilde{F}_N$ is not unique, however. For example, it is possible, and perhaps more natural, to replace $f(q^2)$ by unity in (3.7), obtaining

$$\tilde{F}_N=g^N\int_0^1\prod_{i=1}^{N}[dx_i(1-x_i)^{\alpha_0-1}]\times w^{-\alpha_0-5/6}q^{-1/3}\prod_{i<j}\tilde{\psi}(C_{ji})^{-p_i\cdot p_j}. \tag{3.9}$$

With this definition, the integrand involves elementary functions only.

## IV. NONORIENTABLE DIAGRAMS

Diagrams containing loops with an odd number of twists are called nonorientable. This is because of the dual diagram surface.[15] If one draws such a loop in terms of quark lines, then one finds two quarks circulating around the nonorientable loop in the same direction. Restricting to mesons, such diagrams have no correspondence with the quark model. This had led the authors of Ref. 16 to suggest that when internal quantum numbers are added to the theory in a suitable fashion, these diagrams give no contribution. Here we restrict ourselves to a theory of external scalar mesons, with no internal symmetry, in which case the nonorientable diagrams are manifestly nonvanishing. Also, as we shall see in Sec. VI, these diagrams are required for unitarity.

The trace calculation and momentum integrations are performed just as in Sec. III. For concreteness, let us consider the case of $M$ adjacent twists discussed in Sec. II. We then have

$$F_{N,M}=4\pi^2 g^{N+M}\int\prod_{i=1}^{N}dv_i\prod_{j=1}^{M}du_j\frac{(1+w)^2w^{-\alpha_0-1}}{\ln^2 w}\times[f(-w)]^{-4}[(1-u_Mv_1\cdots v_Nu_1)\times\prod_{j=1}^{M-1}(1-u_ju_{j+1})\prod_{i=1}^{N}(1-v_i)]^{\alpha_0-1}\times\prod_{i<j}[\psi_N(C_{ji})\text{ or }\psi_{NT}(C_{ji})]^{-p_i\cdot p_j}. \tag{4.1}$$

The functions $\psi_N$ and $\psi_{NT}$, which differ from $\psi$ by some strategic minus signs, are discussed in the Appendix. The subscript $N$ denotes "nonorientable" and the subscript $T$ denotes "twisted." The rule for choosing the appropriate function is the following: $C_{ji}$ denotes the product of the $u$'s and $v$'s appearing between $p_i$ and $p_j$. If there are an even number of $u$'s (twisted lines) use $\psi_N$, whereas if there are an odd number use $\psi_{NT}$. As we are considering diagrams with an odd number of twists, the identity $\psi_N(x)=\psi_{NT}(w/x)$, proved in the Appendix, ensures that the result does not depend on which of the two possible products of $u$'s and $v$'s we choose.

It is also shown in the Appendix that the functions

$$\tilde{\psi}_N=\frac{-2\ln w}{\pi}\sin\left(\frac{\pi\ln x}{2\ln w}\right) \tag{4.2a}$$

and

$$\tilde{\psi}_{NT}=\frac{-2\ln w}{\pi}\cos\left(\frac{\pi\ln x}{2\ln w}\right) \tag{4.2b}$$

differ from $\psi_N$ and $\psi_{NT}$, as $w\to 1$, by $O(q_N^2)$, where

$$q_N=-i\exp(\pi^2/2\ln w).$$

The term $[f(-w)]^{-4}$ diverges near $w\to 1$ like $q_N^{-1/3}$. Therefore, just as in the planar case, we construct a counterterm $\tilde{F}_{N,M}$ that cancels the divergence of $F_{N,M}$ by replacing $\psi_N$ and $\psi_{NT}$ by $\tilde{\psi}_N$ and $\tilde{\psi}_{NT}$, respectively. This rule is also satisfactory in its duality and analyticity properties. This nonorientable counterterm, just as the planar one, is nonunique; one can easily add to it an additional finite counterterm.

The nonorientable loop integrals have an additional interesting property that will prove quite useful in the discussion of unitarity in Sec. VI. Namely, there is a natural way to decompose the integration region into pieces corresponding to different diagrams. We now

[15] K. Kikkawa, S. Klein, B. Sakita, and M. Virasoro, Phys. Rev. D 1, 3258 (1970).

[16] M. B. Halpern, S. Klein, and J. Shapiro, Phys. Rev. 188, 2378 (1969).

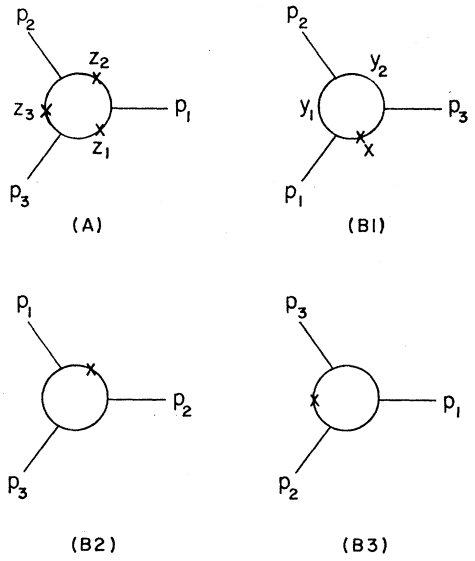


FIG. 4. Equivalent forms for a particular nonorientable loop diagram.

show how this works for a particular example and then state the general rule without further proof.

Consider the diagram labeled configuration $A$ in Fig. 4. According to the rules we have formulated, the integral associated with this diagram is

$$F_A=4\pi^2g^3\int dz_1dz_2dz_3\frac{(1+w)^2[f(-w)]^{-4}}{\ln^2 w}w^{-\alpha_0-1}$$
$$\times[(1-z_1z_2)(1-z_2z_3)(1-z_3z_1)]^{\alpha_0-1}$$
$$\times\psi_N(z_1z_3)^{-p_1\cdot p_2}\psi_{NT}(z_1)^{-p_1\cdot p_3}\psi_N(z_1z_2)^{-p_2\cdot p_3}. \quad (4.3)$$

Now consider the diagrams labeled configurations $B_1$, $B_2$, and $B_3$ in Fig. 4. The diagram $B_i$ can be obtained from configuration $A$ by dualizing the line $z_i$. Therefore, these diagrams should give the same integrals as $A$. To check this property consider $B1$,

$$F_{B1}=4\pi^2g^3\int dxdy_1dy_2\frac{(1+w)^2[f(-w)]^{-4}}{\ln^2 w}w^{-\alpha_0-1}$$
$$\times[(1-y_1)(1-y_2)(1-wx)]^{\alpha_0-1}$$
$$\times\psi_N(y_1)^{-p_1\cdot p_2}\psi_{NT}(x)^{-p_1\cdot p_3}\psi_N(y_2)^{-p_2\cdot p_3}. \quad (4.4)$$

It is obvious that the equality of $F_A$ and $F_{B1}$ (as well as their counterterms) is demonstrated by the change of variables

$$x=1/z_1, \quad y_1=z_1z_3, \quad y_2=z_1z_2. \quad (4.5)$$

This requires the identity $\psi_{NT}(x)=\psi_{NT}(1/x)$, proved in the Appendix. The striking fact is that the integration region of the full expression,

$$z_1, z_2, z_3\geqslant 0; \quad z_1z_2, z_2z_3, z_3z_1\leqslant 1,$$

can be decomposed into the four pieces

$$A: \quad 0\leqslant z_1, z_2, z_3\leqslant 1,$$
$$B_i: \quad 0\leqslant 1/z_i, \ z_iz_{i+1}, z_iz_{i+1}\leqslant 1, \quad i=1, 2, 3$$

which are naturally identified with the four diagrams of Fig. 4 in the way indicated. In other words, the full duality integral can be decomposed into a sum of the four pieces obtained by taking each of the four diagrams with its natural integration variables restricted to the range 0 to 1.

The generalization of the above result to $N$ external lines is as follows: Corresponding to a particular nonorientable one-loop diagram, there are $2^{N-1}$ equivalent configurations obtainable by duality transformations, provided we only consider diagrams with the external lines connected directly to the loop, i.e., diagrams of the general form considered in Sec. II. The integral corresponding to any one of these diagrams is the same, but can be expressed as a sum of $2^{N-1}$ terms corresponding to the various configurations with the integrals in each case restricted to the "unit cube," i.e., with the integration for each of the natural variables running from 0 to 1. The advantage of this decomposition is that each of the "cube-restricted diagrams" only has normal-threshold cuts in the channels that explicitly display them. This result is extremely useful when we examine the unitarity of the loops in Sec. VI.

## V. ORIENTABLE NONPLANAR DIAGRAMS

Diagrams with an even number of twists (greater than zero) have some very startling features. In order to study these features we begin, as before, by writing down the general form of the orientable one-loop integral in the case of $M$ adjacent twists,

$$F_{N,M}=4\pi^2g^{N+M}\int(\prod_{i=1}^{N}dv_i\prod_{j=1}^{M}du_j)$$
$$\times(1-w)^2\frac{f(w)^{-4}}{\ln^2 w}w^{-\alpha_0-1}[(1-u_Mv_1\cdots v_Nu_1)$$
$$\times\prod_{j=1}^{M-1}(1-u_ju_{j+1})\prod_{i=1}^{N}(1-v_i)]^{\alpha_0-1}$$
$$\times\prod_{i<j}[\psi(C_{ji}) \text{ or } \psi_T(C_{ji})]^{-p_i\cdot p_j}. \quad (5.1)$$

$\psi$ is used when an even number of twisted lines are included between $p_i$ and $p_j$ and $\psi_T$ (another function described in the Appendix) is used for an odd number. Once again, the symmetries $\psi(x)=\psi(w/x)$ and $\psi_T(x)=\psi_T(w/x)$ (shown in the Appendix) prevent the formula from depending on which set of included lines is chosen.

The new problems associated with these diagrams can be illustrated by the example shown in Fig. 5(a).

The corresponding integral is

$$F_a=4\pi^2g^4\int d^4x(1-w)^2\frac{[f(w)]^{-4}}{\ln^2 w}w^{-\alpha_0-1}$$
$$\times[(1-x_1x_2)(1-x_2x_3)(1-x_3x_4)(1-x_4x_1)]^{\alpha_0-1}$$
$$\times\psi_T(x_2)^{-p_1\cdot p_2}\psi(x_2x_3)^{-p_1\cdot p_3}\psi_T(x_1)^{-p_1\cdot p_4}$$
$$\times\psi_T(x_3)^{-p_2\cdot p_3}\psi(x_3x_4)^{-p_2\cdot p_4}\psi_T(x_4)^{-p_3\cdot p_4}. \quad (5.2)$$

The integral $F_a$ is invariant under two types of variable changes:

$$x_1'=x_1w, \quad x_2'=x_2/w, \quad x_3'=x_3w, \quad x_4'=x_4/w \quad (5.3)$$

and

$$x_1'=1/x_1, \quad x_2'=w/x_2, \quad x_3'=1/x_3, \quad x_4'=x_4/w.$$

The additional symmetry $\psi_T(x)=\psi_T(1/x)$ is shown in the Appendix. This invariance is important because these transformations allow one to see that the "naive" integration region

$$x_i>0, \quad x_ix_{i+1}<1, \quad i=1,2,3,4$$

can be divided into an infinite number of cells, each of which contributes equally. (Hence the integrals are divergent in a rather trivial way.) The source of this circumstance can be traced to the fact that a sequence of duality transformations can be applied to Fig. 3(a) so as to return it to the original configuration while at the same time inducing one of the changes of variables of (5.3). The upshot of this is that the absorptive parts one might naively have hoped to incorporate in these integrals are in fact counted over and over again an infinite number of times. (This has also been noted by Kaku and Thorn.[8]) The integral with the correct absorptive parts can be obtained by restricting the integration to a single one of the cells.

Consider now the configuration of Fig. 5(b), which can be obtained from Fig. 5(a) by dualizing the line $x_2$. The corresponding integral is given by

$$F_b=4\pi^2g^4\int d^2u\,d^2v(1-w)^2\frac{[f(w)]^{-4}}{\ln^2 w}w^{-\alpha_0-1}$$
$$\times[(1-u_1)(1-u_2)(1-v_1u_2v_2)(1-v_2u_1v_1)]^{\alpha_0-1}$$
$$\times\psi_T(v_1)^{-p_1\cdot p_2}\psi(u_2)^{-p_1\cdot p_3}\psi_T(u_1v_1)^{-p_1\cdot p_4}$$
$$\times\psi_T(v_1u_2)^{-p_2\cdot p_3}\psi(u_1)^{-p_2\cdot p_4}\psi_T(v_2)^{-p_3\cdot p_4}. \quad (5.4)$$

Using the relation $\psi_T(x)=\psi_T(1/x)$, the equality of (5.2) and (5.4) is made manifest through the change of variables

$$x_1=u_1v_1, \quad x_2=1/v_1, \quad x_3=v_1u_2, \quad x_4=v_2. \quad (5.5)$$

A similar transformation takes one to the configuration of Fig. 5(c). Now suppose we restrict the integration for each of the three diagrams to a unit (four-dimensional)

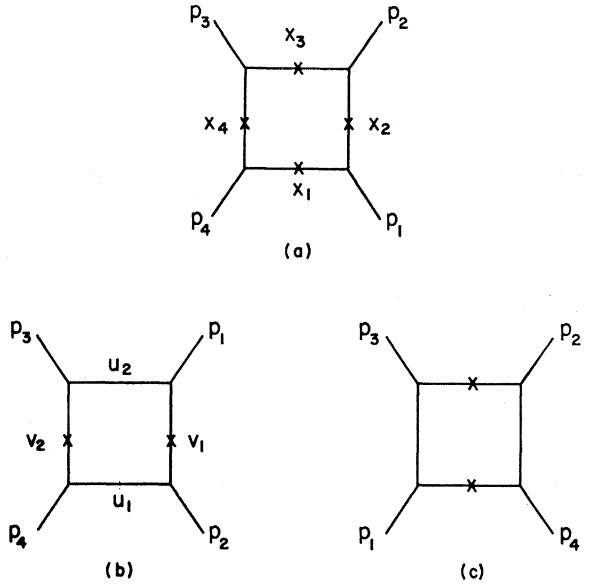


FIG. 5. Equivalent forms for a particular orientable nonplanar loop diagram.

cube. It is then evident that the three regions so defined are disjoint when expressed in terms of the $x$ variables. Furthermore, they remain disjoint even when one allows for the transformations of (5.3). In fact, taken together these three regions precisely define a cell which, with its images obtained by repeated application of (5.3), fill up the original integration region. The general rule, identical to the nonorientable case (and trivially to the planar as well), is to take each of the different loop configurations (of the form of Fig. 2) that can be reached by duality transformations of a particular diagram and restrict the integrations to the cubes defined by having the "natural" variables go from 0 to 1. Diagrams related by duality transformations can then be combined into one with an appropriately enlarged integration region, which in fact is the basic cell corresponding to the invariances of the type shown in (5.3).

We now turn to the question of renormalization. We recall that in the examples of Secs. III and IV the integrals contained an exponential divergence for $w\to 1$, which was entirely due to the factor $[f(\pm w)]^{-4}$. The properties of $\psi$, $\psi_N$, and $\psi_{NT}$ turned out to make possible the subtraction of an appropriately defined counterterm so as to obtain a well-defined and physically sensible result. The orientable nonplanar diagrams which we are considering now are the only one-loop diagrams that contain the function $\psi_T$. As is shown in the Appendix, this function differs in a fundamental way from the other three. Namely, in the limit $w\to 1$ it contains an exponentially behaved factor of $q^{-1/4}$. As a result of this the exponential behavior of the integrand near $w=1$ has additional important contributions. In fact, it is easily seen that the principal behavior

of the integrand near $w=1$ is given by $q^{-1/3-u/4}$, where $u$ is the channel with the double pole in the example of Fig. 5. More generally, for a diagram of this class the lines are always composed of two well-defined sets corresponding to the two windows of the dual surface.[15] Or, put in simpler language, when drawn with quark lines there is one channel that has no quark lines running across it; i.e., the diagram can be pulled apart without breaking any quark lines. This serves to single out a particular channel called $u$. This channel is naturally identified as carrying vacuum quantum numbers only.

We have seen that the integrand has leading behavior near $w \to 1$ of the form $q^{-1/3-u/4}$. Expanding out the integrand in powers of $q$, it also contains less singular terms $q^{-1/3-u/4+n}$, $n=1, 2, \ldots$. It therefore follows that any diagram of this class is well-defined (convergent) for $u<-\frac{4}{3}$, and contains singularities for

$$u=-\tfrac{4}{3}+4n, \quad n=0, 1, 2, \ldots. \tag{5.6}$$

These singularities turn out to be logarithmic branch points. It is remarkable that their position is independent of $\alpha_0$. If one naively attempts to construct a counterterm in the same way as in Sec. IV (as one probably should) one would subtract a term with $\psi$ replaced by $\tilde{\psi}$ and $\psi_T$ replaced by

$$\tilde{\psi}_T=-[(\ln w)/2\pi]q^{-1/4}.$$

This would remove the branch point at $u=-\frac{4}{3}$, but all the higher ones would still survive.

The branch points we have just found are quite peculiar. They do not correspond to normal thresholds and they only occur in vacuum quantum numbers. Furthermore, they have definite angular momentum properties, lying, in fact, on a new kind of Regge cut. Since the branch point at $u=-\frac{4}{3}+4n$ contains angular momentum $n, n-2, \ldots, 0$ (for $n$ even), it would seem that the $J$-plane cut trajectory is

$$\alpha_{\text{cut}}(u)=\tfrac{1}{3}+\tfrac{1}{4}u. \tag{5.7}$$

In fact, this result is verified by analyzing the asymptotic behavior of these diagrams. Notice that the slope of this Regge cut (just as in the case for the more familiar ones in the crossed channels) is half of the slope of the input pole trajectories of the model. There is a strong temptation to call these cuts the Pomeranchukon and be very happy. However, at least to the present order in $g^2$, these singularities are unacceptable, since they apparently lead to a violation of unitarity. One might hope to find a procedure that eliminates these unwanted singularities from the physical sheet, perhaps at the same time introducing still another $J$-plane singularity related to the Pomeranchukon. Alternatively, the problem may be resolved when higher-order loops are included. We consider this to be an extremely important problem.

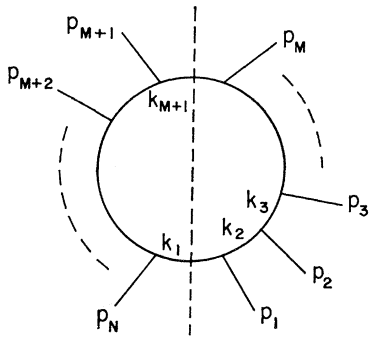


FIG. 6. $(M+N)$-point loop diagram whose absorptive part is examined in the indicated channel.

We should finally remark that cutting out the singular portion of the integration with a factor $\theta(1-w-\epsilon)$ removes the new branch points without altering the other absorptive parts. This kind of cutoff, however, in general leads to an unacceptable asymptotic behavior for the amplitudes. Nevertheless, as an interim measure, such a cutoff should be implicitly understood to be made for this class of diagrams in the discussions of the next section.

## VI. ONE-LOOP UNITARITY

In this section we wish to make a modest beginning on the important question of unitarity. Clearly all the labors of the previous sections are of interest only if one can eventually enumerate an infinite set of diagrams whose sum is unitary. It should be emphasized that *a priori* it is not at all evident that any such selection of dual Feynman graphs can be made. Indeed, it could conceivably turn out that any set of dual Feynman diagrams, having the correct absorptive parts in a particular chosen channel, is not crossing symmetric (i.e., unitary in crossed channels as well). We shall partially answer this question by displaying a selection of $N$-point one-loop diagrams that is both unitary (in a perturbative sense) and crossing symmetric. For simplicity we only deal with connected diagrams. The connectedness structure of the $S$ matrix is a standard problem, relevant for unitarity, but probably not the source of any serious difficulties.

The counting of dual Feynman diagrams with specific absorptive parts can be a rather tricky business because of their tendency to contain cuts in channels that are not manifest when the diagram is drawn in a particular way. For this reason, it turns out to be very useful, as an intermediate step in the discussion, to deal with "maximal-loop diagrams restricted to cubes." By "maximal-loop" we mean that the diagrams are drawn as one large loop with the external scalar states directly attached, as in Fig. 1. "Restriction to cubes" means that when the integration variables are introduced in the natural way described in Sec. II, the integrals are restricted to the region defined by the unit cube of these variables. This is just the sort of term we obtained by decomposing diagrams in Secs.

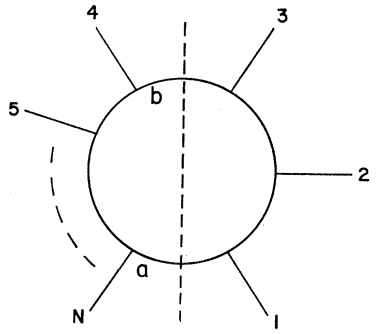


FIG. 7. Absorptive part of an $N$-point loop diagram in a three-body channel.

IV and V. It is important to remember that when an integration is restricted in this way, a twisted line may not be dualized.

We now state the rule for obtaining a unitary expression: For a particular ordering of the $N$ external momenta, sum the $2^N$ terms obtained by allowing each of the $N$ internal lines to be either twisted or untwisted. Then sum all inequivalent permutations of the external momenta. This gives a total of $2^{N-1}(N-1)!$ terms, each of which is a maximal-loop integral restricted to a cube. With this rule at hand we proceed to indicate why, aside from the spurious singularities found in Sec. V, the only absorptive parts of this sum of terms are the usual two-particle thresholds, and why the corresponding discontinuities are the appropriate products of $M+2$ and $N-M+2$ particle trees (see Fig. 6) integrated over two-body phase space.

The advantage of integrals restricted to cubes is that they only contain cuts in channels that are manifest as drawn. Therefore, to consider the absorptive part in a particular channel we may consider the subset of diagrams having the lines appropriately divided into two sets. Thus the $M$ lines on the right in Fig. 6 may be arbitrarily permuted and similarly for the $N-M$ lines on the left. For a particular assignment of twists, we recall (in rather schematic form) the formula of Sec. II,

$$\int d^4k \int_0^1 \prod_{i=1}^{N} [du_i u_i^{-\alpha(k_i^2)-1}] \times(1\pm w)^2[G(u_1, u_2, \ldots, u_N)]^{\alpha_0-1} \times \mathrm{Tr}\{V(\pm u_1)^R V(\pm u_2)^R \cdots V(\pm u_N)^R\},$$

where the signs and $G$ are chosen in accordance with the rules of Sec. II. To investigate the discontinuity across the two-body cut for which internal line No. 1 is in the state $|s\rangle$ and internal line No. $M+1$ is in the state $|s'\rangle$, one simply inserts $|s\rangle\langle s|$ and $|s'\rangle\langle s'|$ into the appropriate locations of the trace. Also, if these two states have $R|s\rangle=r|s\rangle$ and $R|s'\rangle=r'|s'\rangle$, one replaces ${u_1}^{R-\alpha(k_1^2)-1}$ by $\delta(r-\alpha(k_1^2))$, putting $u_1=0$ elsewhere and dropping the $u_1$ integration. Similarly, ${u_{M+1}}^{R-\alpha(k_{M+1}^2)-1}$ is replaced by $\delta(r'-\alpha(k_{M+1}^2))$. This rule is just the natural analog of the Cutkosky prescription. It is somewhat oversimplified as stated because $|s\rangle$ and $|s'\rangle$ need not be eigenstates of $R$ (whenever $\alpha_0\neq 1$), but the generalization can be easily made. After carrying out the indicated substitutions, one is left with a two-dimensional phase-space integration (of the usual type) of the product of two tree diagrams, just as desired.

To complete the demonstration that the two-body discontinuity is correct, we should show that the sum of all the terms contributing on either side of a particular discontinuity is, in fact, the appropriate $N$-point function. The delicate point is that when any line is twisted, the corresponding factor in the discontinuity is *not* an $N$-point tree. Rather, because of the way in which the integration regions have been restricted, it is only part of a tree. Remarkably, all the terms combine to give precisely the desired sum of trees. Rather than proving this fact in all generality, we demonstrate it for a specific example.

Consider a discontinuity of the type shown in Fig. 7. For simplicity we shall take $a$ and $b$ to be ground states. Then, when all terms are summed, we expect to get as one factor the sum of all five-point trees made from particles $a$, $b$, 1, 2, and 3. There are 12 such trees. To obtain these 12 trees we must combine the 24 terms arising from the six permutations of particles 1, 2, and 3 and the four possible twist combinations for the two internal lines between them. The six terms with no twists are six of the desired trees. The remaining six trees are obtained by combining the other 18 terms in appropriate fashion.

To see how the remaining terms are combined, consider the diagrams shown in Fig. 8. Any one of

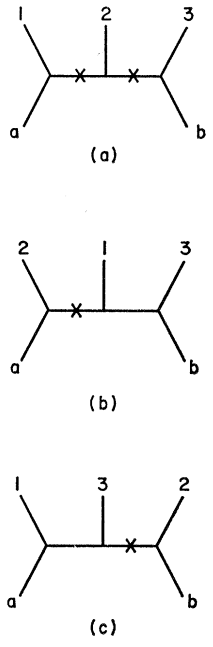


FIG. 8. Three equivalent five-point functions.

these terms would represent the same tree if the integration limits were appropriate. However, the integration limits emerging from factorizing terms restricted to cubes are only portions of tree diagrams. In fact, the three terms in Fig. 8 combine to give the complete tree corresponding to any one of them. In this way, the 18 terms with twists give the six remaining trees. Let us sketch how the algebra works. Corresponding to Fig. 8(a), we obtain

$$F_a = g^3 \int_0^1 dx_1 dx_2 x_1^{-\alpha_{a1}-1} x_2^{-\alpha_{3b}-1} (1+x_1)^{-p_1\cdot p_2} \times (1+x_2)^{-p_2\cdot p_3} (1-x_1x_2)^{\alpha_0-1-p_1\cdot p_3}$$

$$= g^3 \int_0^1 dx_1 dx_2 I(x_1,x_2).$$

On the other hand, Fig. 6(b) gives

$$F_b = g^3 \int_0^1 dy_1 dy_2 y_1^{-\alpha_{a2}-1} y_2^{-\alpha_{3b}-1} (1+y_1)^{-p_1\cdot p_2} \times (1-y_2)^{-\alpha_{13}-1} (1+y_1y_2)^{-p_2\cdot p_3}.$$

The change of variables $y_1 = 1/x_1$, $y_2 = x_1x_2$ brings $F_b$ to the form

$$F_b = \int_{x_1>1,\, x_1x_2<1} I(x_1,x_2) dx_1 dx_2.$$

In similar fashion, the diagram in Fig. 8(c) contributes

$$F_c = \int_{x_2>1,\, x_1x_2<1} I(x_1,x_2) dx_1 dx_2.$$

Thus the three terms combine to give the complete five-point function

$$F = \int_0^\infty dx_1 dx_2 \theta(1-x_1x_2) I(x_1,x_2).$$

(A change of variables is still required to obtain the Bardakci-Ruegg form.) Not surprisingly, the corresponding algebra can be carried through for the general case.

As an additional comment, we point out that there are actually four terms of each type, which differ only in the twistedness of lines $a$ and $b$, and thus superficially appear to contribute equally to the absorptive parts. Two of these terms are orientable and two are nonorientable. It is important to include all four terms in order that the intermediate states producing threshold branch points all have physical signature.

We have now shown that a certain manifestly crossing-symmetric sum of terms comprises the complete one-loop contribution to the connected part of the unitary $S$ matrix. It is important for several reasons to reassemble these diagrams as dual Feynman diagrams with the complete integration regions instead of the cube restrictions. First of all, this will lead to a simpler counting of diagrams and allow the dualization of any line, twisted or not. Secondly, the elimination of spurious states by means of projections in Sec. II was carried out for complete diagrams. When the diagrams are decomposed into cubes the individual terms will have absorptive parts corresponding to spurious intermediate states. If these spurious-particle thresholds are to be absent from the complete answer, it is important that the sum or diagrams can be expressed as a sum of complete duality diagrams without any pieces left over.

The identification of complete dual Feynman diagrams from the $2^{N-1}(N-1)!$ cube-restricted diagrams is actually quite easy using the rules of Secs. IV and V. The $(N-1)!/2$ terms without twists give directly the $(N-1)!/2$ inequivalent planar terms. These are related by duality transformations to the diagrams obtained by attaching the tadpole of Fig. 1(a) to each of the possible $N$-point tree diagrams. The $2^{N-2}(N-1)!$ terms with an odd number of twists are readily combined to give the $(N-1)!/2$ inequivalent nonorientable terms. These are related by duality transformations to the diagrams obtained by attaching the tadpole of Fig. 1(b) to each of the $N$-point tree diagrams. Finally, there are the terms with an even number of twists. These may also be combined to give complete duality diagrams. They may be related to the diagrams obtained by inserting the self-energy of Fig. 1(c) onto some line (external or internal) of a tree. If this insertion is made so as to divide the external lines into a set of $M$ lines (containing a particular one) and $N-M$ lines, then, for $N>4$, there are $(N-1)!/2(N-M)$ inequivalent diagrams of this type. This completes the classification of one-loop diagrams. We have found that a unitary answer requires adding each inequivalent dual Feynman diagram with equal weight, a remarkably simple result.

## VII. CONCLUSIONS

We have given the rules for the explicit calculation of all one-loop dual Feynman diagrams with any number of twisted lines. These are expressed as integrals involving elliptic functions. The planar and the nonorientable diagrams were renormalized. We showed that the nonplanar orientable diagrams develop new singularities which are perhaps associated with the Pomeranchuk trajectory. Finally, we showed that the sum of all inequivalent dual Feynman diagrams, taken with equal weights, is unitary to this order of the perturbation series.

Let us now review the current stage of development of the theory and the problems that remain to be solved before a dual unitary theory can be written down. The analysis of the structure of dual Feynman graphs that we have given in Ref. 11 showed that all dual graphs could be constructed with the aid of the operators

corresponding to the four one-particle irreducible graphs of the theory (see Fig. 1). Three of these operators [Figs. 1(a)–1(c)] are one-loop operators and can therefore be constructed explicitly by factorizing the expressions we have given for the $N$-particle one-loop diagrams into a product of trees and the appropriate one-loop operator.[17] In Ref. 10 we explicitly calculated the renormalized planar self-energy operator from a knowledge of the planar one-loop diagrams and their renormalization. It is not difficult to extract the planar tadpole operator [Fig. 1(a)], which can then be used in conjunction with the general vertex operator to construct all multiloop planar diagrams. (The self-energy operator can also be used directly.) The formulas of this paper allow one to construct, by techniques completely analogous to those of Ref. 10, the operators corresponding to Figs. 1(b) and 1(c) as well. In each case a reasonable counterterm operator is obtained by replacing the various $\psi$ functions by the corresponding $\tilde{\psi}$ functions. Whether this prescription is valid for the self-energy operator of Fig. 1(c) remains to be seen.

The remaining problems in the implementation of the unitarization program are the following.

(1) One must deal with the new singularities generated by the nonplanar orientable graphs and perhaps relate them to the Pomeranchukon.

(2) The operator corresponding to Fig. 1(d) still needs to be constructed. Although we can write the operator expression for this graph, its explicit evaluation is quite difficult. Note that its renormalization is related to the renormalization of the nonplanar orientable graph because it contains this graph as a factor when two internal lines are cut.

(3) One must study the new divergences that appear when any of the four primitive renormalized operators is iterated.

(4) Consistency conditions and other criteria that may bear on the uniqueness of the procedure used to construct counterterms require further investigation.

(5) Once the above problems have been resolved, any given dual Feynman diagram can be constructed by iteration of the primitive operators. It then remains to determine the relative weights of the various terms in the perturbation series such that the resulting sum is perturbatively unitary. It is possible that one could then exhibit explicit integral equations which sum the complete set of diagrams. We have found that each inequivalent one-loop graph should be included with equal (unit) weight. It is perhaps reasonable to conjecture that a similar rule is also valid for multiloop graphs.

## ACKNOWLEDGMENT

We wish to acknowledge gratefully the participation of Dr. T. H. Burnett in the early stages of this work.

[17] The details of this construction and the forms of the primitive operators will be given elsewhere.

## APPENDIX

In the text we were led to introduce the following four functions:

$$\psi(x)=-2\pi i\exp\left(\frac{\ln^2 x}{2\ln w}\right)\times\theta_1\left(\frac{\ln x}{2\pi i}\middle|\frac{\ln w}{2\pi i}\right)\Big/\theta_1'\left(0\middle|\frac{\ln w}{2\pi i}\right),\quad\text{(A1)}$$

$$\psi_N(x)=-2\pi i\exp\left(\frac{\ln^2 x}{2\ln w}\right)\times\theta_1\left(\frac{\ln x}{2\pi i}\middle|\frac{\ln w}{2\pi i}+\frac{1}{2}\right)\Big/\theta_1'\left(0\middle|\frac{\ln w}{2\pi i}+\frac{1}{2}\right),\quad\text{(A2)}$$

$$\psi_{NT}(x)=-2\pi i\exp\left(\frac{\ln^2 x}{2\ln w}\right)\times\theta_1\left(\frac{\ln x}{2\pi i}+\frac{1}{2}\middle|\frac{\ln w}{2\pi i}+\frac{1}{2}\right)\Big/\theta_1'\left(0\middle|\frac{\ln w}{2\pi i}+\frac{1}{2}\right),\quad\text{(A3)}$$

$$\psi_T(x)=2\pi\exp\left(\frac{\ln^2 x}{2\ln w}\right)\times\theta_1\left(\frac{\ln x}{2\pi i}+\frac{1}{2}\middle|\frac{\ln w}{2\pi i}\right)\Big/\theta_1'\left(0\middle|\frac{\ln w}{2\pi i}\right).\quad\text{(A4)}$$

$\theta_1(\nu|\tau)$ is a standard Jacobi $\theta$ function in the notation of the Bateman project. In each case we require an accurate asymptotic estimate of the function for $w\to 1$. For this purpose one requires the transformation formula

$$\theta_1\left(\frac{\nu}{\alpha+\beta\tau}\middle|\frac{\gamma+\delta\tau}{\alpha+\beta\tau}\right)=\epsilon(\alpha+\beta\tau)^{1/2}\times\exp\left(\frac{i\pi\beta\nu^2}{\alpha+\beta\tau}\right)\theta_1(\nu|\tau),\quad\text{(A5)}$$

where $\epsilon^8=1$ and $\alpha$, $\beta$, $\gamma$, and $\delta$ are integers satisfying $\alpha\delta-\beta\gamma=1$.

For the first function, $\psi(x)$, we choose $\alpha=\delta=0$ and $\gamma=-\beta=1$ to show that

$$\psi(x)=-\ln w\,\theta_1\left(\frac{\ln x}{\ln w}\middle|\frac{-2\pi i}{\ln w}\right)\Big/\theta_1'\left(0\middle|\frac{-2\pi i}{\ln w}\right)$$
$$=-\frac{\ln w}{\pi}\sin\left(\frac{\pi\ln x}{\ln w}\right)\times\prod_{n=1}^{\infty}\left[\frac{1-2q^{2n}\cos(2\pi\ln x/\ln w)+q^{4n}}{(1-q^{2n})^2}\right],\quad\text{(A6)}$$

where

$$q=e^{2\pi^2/\ln w}.$$

This formula provides an extremely good estimate of $\psi(x)$ near $w=1$. We see that $\psi(x)$ differs from

$$\tilde{\psi}(x)=\frac{-\ln w}{\pi}\sin\left(\frac{\pi \ln x}{\ln w}\right) \tag{A7}$$

only by $O(q^2)$. The identity

$$\psi(x)=\psi(w/x) \tag{A8}$$

is also manifest in (A6).

For the second function, $\psi_N(x)$, the choice $\beta=-2$, $\gamma=0$, $\alpha=\delta=1$ in (A5) and some simple manipulations allow one to show

$$\psi_N(x)=-2\ln w\,\theta_1\left(\frac{\ln x}{2\ln w}\middle|-\tfrac{1}{2}-\frac{\pi i}{2\ln w}\right)\Big/\theta_1'\left(0\middle|-\tfrac{1}{2}-\frac{\pi i}{2\ln w}\right)$$
$$=-\frac{2\ln w}{\pi}\sin\left(\frac{\pi \ln x}{2\ln w}\right)\times\prod_{n=1}^{\infty}\left[\frac{1-2q_N{}^{2n}\cos(\pi \ln x/\ln w)+q_N{}^{4n}}{(1-q_N{}^{2n})^2}\right], \tag{A9}$$

where

$$q_N=-ie^{\pi^2/2\ln w}.$$

From Eq. (A9) it is clear that

$$\tilde{\psi}_N(x)=-\frac{2\ln w}{\pi}\sin\left(\frac{\pi \ln x}{2\ln w}\right) \tag{A10}$$

differs from $\psi_N(x)$ by $O(q_N{}^2)$ as $w\to 1$. The symmetry

$$\psi_N(x)=-\psi_N(1/x) \tag{A11}$$

is also evident.

For the third function, $\psi_{NT}(x)$, one uses the same transformation formula as for $\psi_N(x)$, together with additional identities

$$\theta_1(\nu\,|\,\tau)=-e^{-i\tau(2\nu-\tau)}\theta_1(\nu-\tau\,|\,\tau) \tag{A12}$$

and

$$\theta_1(\tfrac{1}{2}-\nu\,|\,\tau)=\theta_2(\nu\,|\,\tau) \tag{A13}$$

to show that

$$\psi_{NT}(x)=2\ln w\,\theta_2\left(\frac{\ln x}{2\ln w}\middle|-\tfrac{1}{2}-\frac{\pi i}{2\ln w}\right)\Big/\theta_1'\left(0\middle|-\tfrac{1}{2}-\frac{\pi i}{2\ln w}\right)$$
$$=-\frac{2\ln w}{\pi}\cos\left(\frac{\pi \ln x}{2\ln w}\right)\times\prod_{n=1}^{\infty}\left[\frac{1+2q_N{}^{2n}\cos(\pi \ln x/\ln w)+q_N{}^{4n}}{(1-q_N{}^{2n})^2}\right]. \tag{A14}$$

Comparing (A9) and (A14) gives the additional symmetries

$$\psi_{NT}(x)=\psi_N(w/x),\quad \psi_{NT}(x)=\psi_{NT}(1/x). \tag{A15}$$

Also, the function

$$\tilde{\psi}_{NT}(x)=-2\frac{\ln w}{\pi}\cos\left(\frac{\pi \ln x}{2\ln w}\right) \tag{A16}$$

agrees with $\psi_N(x)$ to $O(q_N{}^2)$ for $w\to 1$.

Finally, for $\psi_T(x)$, we use the same transformation formula as for $\psi(x)$ together with the identity

$$\theta_1(\nu+\tfrac{1}{2}\tau\,|\,\tau)=ie^{-i\pi(\nu+\tau/4)}\theta_4(\nu\,|\,\tau) \tag{A17}$$

to deduce that

$$\psi_T(x)=-\ln w\,\theta_4\left(\frac{\ln x}{\ln w}\middle|-\frac{2\pi i}{\ln w}\right)\Big/\theta_1'\left(0\middle|-\frac{2\pi i}{\ln w}\right)$$
$$=-\tfrac{1}{2}\ln w q^{-1/4}\times\prod_{n=1}^{\infty}\left[\frac{1-2q^{2n-1}\cos(2\pi \ln x/\ln w)+q^{4n-2}}{(1-q^{2n})^2}\right]. \tag{A18}$$

This function has the manifest symmetries

$$\psi_T(x)=\psi_T(1/x)=\psi_T(w/x). \tag{A19}$$

Also, it contains the exponential factor $q^{-1/4}$ and differs from

$$\tilde{\psi}_T(x)=-[(\ln w)/2\pi]q^{-1/4} \tag{A20}$$

by $O(q)$ as $w\to 1$.